Unusually Detailed Insight into the Dynamic Behavior of Coordinated Ambidentate Ligands. Factors Influencing the Binding Mode of 2-Aminopyridines in B_{12} Models

Luigi G. Marzilli,*† Michael F. Summers,†,‡ Ennio Zangrando,§ Nevenka Bresciani-Pahor,§ and Lucio Randaccio*§

Contribution from the Department of Chemistry, Emory University, Atlanta, Georgia 30322, and Dipartimento di Scienze Chimiche, Universita di Trieste, 34127 Trieste, Italy.
Received December 11, 1985

Abstract: Endocyclic N-bound 2-aminopyridine ($2NH_2py$) when coordinated to B_{12} coenzyme models simulates the very long Co–N bonds characteristic of axially bound 5,6-dimethylbenzimidazole in cobalamins. Ambidentate isomerism has now been found for $2NH_2py$ and related ligands coordinated to cobaloximes, $LCo(DH)_2R$ (L = $2NH_2py$ or substituted $2NH_2py$, R = alkyl, DH = monoanion of dimethylglyoxime). Dynamic and saturation transfer ^1H NMR spectroscopy and/or VIS spectrophotometry were employed for rate measurements of (1) rotation about the Co–N bond of endocyclic N-bound $2NH_2py$ derivatives ($k_{rot.}$ = 3.9×10^2 and 1.4×10^4 s^{-1} at −90 °C for L = $2NH_2py$ and R = CH_2NO_2 and i-C_3H_7, respectively), (2) ambidentate isomerization between endocyclic and exocyclic N-binding (k_f(eq 1′) = 7.2×10^{-1} and 2.4×10^2 s^{-1} at 25 °C for L = $2NH_2py$ and R = CH_2CF_3 and $CH_2C(CH_3)(CO_2C_2H_5)_2$, respectively), and (3) dissociation of exocyclic and endocyclic N-bound $2NH_2py$ derivatives. Since, for a given R, the isomerization rate is an order of magnitude greater than the ligand

$$2NH_2pyCo(DH)_2R \underset{k_r}{\overset{k_f}{\rightleftharpoons}} py2NH_2Co(DH)_2R \qquad (1')$$

dissociation rate, isomerization is largely an intramolecular process. Thus an unusually detailed description of the dynamic properties of these $2NH_2py$ compounds has emerged. In addition, the influence of substituents on the $2NH_2py$ ring and on the amino group was investigated, and the results obtained are readily rationalized by electronic or steric effects. The isomerization equilibrium was not influenced by the electron donating ability of R. However, when R was a bulky ligand such as neopentyl, the amino bound ambidentate isomer was favored. To our knowledge, this is the first clear solution evidence of a trans steric influence of R for a B_{12} model system. Such steric interactions are important considerations in the proposed mechanism of action of B_{12} dependent enzymic processes. An additional novel finding in this study was that the position of equilibrium 1′ was shifted to the right on addition of excess $2NH_2py$. Since $2NH_2py$ concentration does not appear in the equilibrium expression, this unexpected result was explored by ^1H NMR spectroscopy. Shifts of the O–H–O signal suggested a H-bonding interaction between the O–H–O group of the amino bound isomer and the amino group of uncoordinated $2NH_2py$. Such an interaction and exocyclic amino group binding were demonstrated in the solid state. The crystal and molecular structures of $py2NH_26NH_2Co(DH)_2CH_2CH_3 \cdot py2NH_26NH_2$ were determined (space group $P\bar{1}$ with a = 9.411 (1) Å, b = 10.276 (1) Å, c = 13.776 (2) Å, α = 102.81 (1)°, β = 99.68 (2)°, γ = 81.85 (1)°, V = 1273.0 Å^3, Z = 2, D_c = 1.40 g/cm^3, D_n = 1.39 g/cm^3, R = 0.043, for 3806 independent reflections). The coordinated $py2NH_26NH_2$ binds via an NH_2 group (Co–N bond = 2.156 (3) Å). The uncoordinated $2NH_26NH_2py$ has short contacts (3.01 and 2.94 Å) between one of the amino N's and the oxime O's of two complexes. Since the endocyclic $2NH_2py$ binding is stabilized by intramolecular H-bonding, the dependence of the position of equilibrium 1′ on excess ligand concentration can be understood as arising from competition between intra- and intermolecular H-bonding.

Very little information exists on the strength of metal-to-carbon bonds. The existence of Co–C bonds in B_{12} coenzymes, coupled with evidence that this bond cleaves homolytically in B_{12} dependent enzymic processes,[1,2] has stimulated investigations into factors influencing Co–C bond strength in cobalamins[3,4] and B_{12} model compounds.[5,6] Employing both equilibrium and kinetic methods, Halpern and co-workers have elucidated factors which influence the Co–C bond dissociation energy as a function of the neutral, trans-axial ligand L in cobaloximes with the formula $LCo(DH)_2R$, where R = organic monoanion and DH = monoanion of dimethylglyoxime.[5]

As models for coenzyme B_{12}, cobaloximes can be faulted on a number of counts including electrochemical,[6] kinetic,[7-9] and structural properties,[7,9-12] The $(DH)_2$ equatorial ligand system is not as electron donating as the corrin in coenzyme B_{12} or the Schiff-base equatorial ligands of other B_{12} models.[5] Compared to both cobalamins[3,4] and other model systems,[3-5,9,10] cobaloximes have stronger Co–C bonds[5] and shorter Co–L bonds.[11] Nevertheless, a large variety of cobaloxime compounds can be synthesized and studied[11] whereas, in other model systems, the variety of reported compounds is considerably smaller.

The understanding of the chemistry of cobalamins requires extensive studies of several types of model systems since the

† Emory.
‡ Present address: Biophysics Laboratory, Office of Biologics Research and Review, Food and Drug Administration, 8800 Rockville Pike, Bethesda, MD 20892.
§ Trieste.

(1) Dolphin, D., Ed. B_{12} (2 volumes); Wiley: New York, 1982.
(2) Pratt, J. M., Ed. *Inorganic Chemistry Of Vitamin B_{12}*; Academic Press: New York, 1972. Babior, B. M.; Krouwer, J. S. *CRC Crit. Rev. Biochem.* **1979**, 35. Toscano, P. J.; Marzilli, L. G. *Prog. Inorg. Chem.* **1984**, *31*, 105. Finke, R. G.; Schiraldi, D. A.; Mayer, B. J. *Coord. Chem. Rev.* **1984**, *54*, 1.
(3) Halpern, J. *Science (Washington, DC)* **1985**, *227*, 869. Halpern, J.; Kim, S.-H.; Leung, T. W. *J. Am. Chem. Soc.* **1984**, *106*, 8317.
(4) Finke, R. G.; Hay, B. P. *Inorg. Chem.* **1984**, *23*, 3041. Hay, B. P.; Finke, R. G. *J. Am. Chem. Soc.*, in press.
(5) Halpern, J., ref 1, Vol. 1, p 501. Ng, F. T. T.; Rempel, G. L.; Halpern, J. *J. Am. Chem. Soc.* **1982**, *104*, 621. Ng, F. T. T.; Rempel, G. L.; Halpern, J. *Inorg. Chim. Acta* **1983**, *77*, L165. Halpern, J. *Pure Appl. Chem.* **1983**, *55*, 1059.
(6) Elliott, C. M.; Hershenhart, E.; Finke, R. G.; Smith, B. L. *J. Am. Chem. Soc.* **1981**, *103*, 5558. Finke, R. G.; Smith, B. L.; Droege, M. W.; Elliott, C. M.; Hershenhart, E. *J. Organomet. Chem.* **1980**, *202*, C25. Finke, R. G.; Smith, B. L.; Mayer, B. J.; Molinero, A. A. *Inorg. Chem.* **1983**, *23*, 3677.
(7) Parker, W. O., Jr.; Bresciani-Pahor, N.; Zangrando, E.; Randaccio, L.; Marzilli, L. G. *Inorg. Chem.* **1985**, *24*, 3908. Marzilli, L. G.; Bresciani-Pahor, N.; Randaccio, L.; Zangrando, E.; Myers, S. A.; Finke, R. G. *Inorg. Chim. Acta* **1985**, *107*, 139.
(8) Milton, P. A.; Brown, T. L. *J. Am. Chem. Soc.* **1977**, *99*, 1390. Reenstra, W. W.; Jencks, W. P. *J. Am. Chem. Soc.* **1979**, *101*, 5780. Brown, K. L.; Awtrey, A. W.; Chock, P. B.; Rhee, S. G. In *Vitamin $B1_2$*; Zagalak, W. F., Ed.; Walter de Gruyter & Co.; New York, 1979.
(9) Summers, M. F.; Marzilli, L. G.; Bresciani-Pahor, N.; Randaccio, L. *J. Am. Chem. Soc.* **1984**, *106*, 4478.

0002-7863/86/1508-4830$01.50/0

differences in properties between the models and cobalamins are instructive. If changes in the nature of the ligands in a particular type of model compound lead to properties more similar to those of cobalamins, then such information is of particular value.

In this vein, Halpern and co-workers have identified cobaloximes with much weaker Co–C bonds.[5] In preliminary studies, these investigators found that some 2XpyCo(DH)$_2$R compounds, where 2Xpy = 2-substituted pyridine, have relatively weak Co–C bonds.[13] Our interest in the relationship of structure to the chemistry of cobaloximes led us to characterize structurally one member of this class of compounds, namely 2NH$_2$pyCo(DH)$_2$-*i*-C$_3$H$_7$, and to examine the solution chemistry of related compounds.[12]

Several interesting features emerged.[12] First, dissociation of the 2NH$_2$py type ligand was relatively fast compared to the basicity of the ligand. This feature is desirable in a B_{12} model since ligand dissociation rates are high in native B_{12} systems.[8] Second, the axial Co–N bond was very long, approaching that found for coenzyme B_{12}[10] and B_{12} models with Schiff-base ligands.[9] Although the relationships between Co–N(axial) bond length and Co–C bond energy are not fully understood,[9] our structural studies on the few systems for which estimates of Co–C bond energies are available indicate that complexes with weak Co–C bonds have long Co–N(axial) bonds.[9,12] Co–C bond lengths can vary but, for R of similar bulk and nonbulky L, Co–C bond lengths appear insensitive to changes in the equatorial ligand for systems examined thus far.[7,9,11]

Bond lengths are obtained for solids, whereas bond energies are estimated for solutions. The 2NH$_2$py ligand is potentially ambidentate, having exocyclic (exo) and endocyclic (endo) N-binding sites. Employing a variety of techniques, we failed to establish the binding mode in solution but were able to conclude that, for the compounds investigated, the endocyclic binding mode was predominant.[12]

Since cobaloximes with 2NH$_2$py more closely approached the structural and bonding characteristics of corrin systems, we decided to explore more deeply the solution chemistry using low-*T*, high-field FT–NMR spectroscopy. This approach has allowed us to gain an unusually detailed knowledge of the dynamic properties of 2-aminopyridine cobaloximes. Thus far we have been able to observe the dependence of ligand rotation rates (rotation about the Co–N bond) as a function of the trans R ligand, to demonstrate that 2NH$_2$py and related ligands are ambidentate, to measure the rate of isomer interconversion, to determine the influences of different R groups and of substituents on 2NH$_2$py on the position of equilibrium, and finally, to demonstrate that the equilibrium position is a function of added 2NH$_2$py. Many of these observations are unprecedented, and, together, they provide unusually detailed information on ligand dynamics. Furthermore, we have obtained the X-ray structure of a complex with an exocyclic N bound 2-aminopyridine, (2,6-diaminopyridine)Co(DH)$_2$CH$_2$CH$_3$·2,6-diaminopyridine. The structure of this adduct lends considerable support to our interpretation of the solution results.

Experimental Section

Reagents. All reagents were from Aldrich and were used without further purification except as follows. Methylene-d_2 chloride was from MSD Isotopes. 2-Amino-5-methylpyridine was from Baker. 2-Amino-6-methylpyridine was recrystallized from CH_2Cl_2 by addition of petroleum ether. Reagents used for rate measurements were purified as described previously.[12]

Instrumentation. Ligand substitution reactions were monitored spectrophotometrically with a Cary 14 for the slow reactions ($k_{obsd} < 1.0\ s^{-1}$) and a Durrum-Gibson D-110 stopped-flow spectrophotometer for the fast reactions. Both instruments were equipped with thermostated compartments at 25.0 ± 0.04 °C. ^{1}H NMR magnetization transfer experiments were carried out on a Nicolet NB-360 (360 MHz) and an IBM WP-200SY (200 MHz) spectrometer equipped with temperature control units which maintained the sample within ±0.5 °C. Dynamic ^{1}H NMR data and all other low-temperature NMR data were obtained with the IBM instrument.

^{1}H NMR Line Shape Measurements. Relevant acquisition parameters, experimental conditions, and methods for line shape analyses have been described previously.[9,14] Line shape measurements (CD_2Cl_2) were made for the oxime O–H–O NMR signals for the Co–N rotation studies (typical temperatures: −85 to −30 °C) and the oxime CH_3 signals for isomerization studies.

^{1}H NMR Magnetization Transfer Experiments. ^{1}H NMR magnetization transfer experiments were carried out by using the procedures described by Martin et al.[15] This method allows the simultaneous determination of longitudinal relaxation rates ($1/T_{1x} = R_x$) and exchange rates (k_x) for exchanging nuclei with k_x/R_x values from 0.2 to 20.

Equilibrium Measurements. Equilibrium concentrations of exocyclic and endocyclic N-bound L were determined from the relative magnitudes of the integrated areas of the oxime O–H–O and CH_3 ^{1}H NMR signals. Some of the data were also analyzed by deconvolution (Nicolet NMRCAP); in all cases the areas obtained by the two methods agreed within experimental error.

Ligand Substitution Rates. Absorbance vs. time data were obtained for the substitution of L from LCo(DH)$_2$R by PBu$_3$(CH$_2$Cl$_2$) as described previously.[12] The pseudo-first-order rate data were treated with the standard integrated expresion for a first-order process by using linear least-squares analysis. Rate constants for an S_N1 LIM mechanism are defined below (eq 1–3). Rate constants for a system undergoing rapid isomerization prior to ligand dissociation are defined in eq 4–8, where pyNH$_2$Co and NH$_2$pyCo represent complexes containing exocyclic and endocyclic N-bound L, respectively, and Co represents the Co(DH)$_2$R moiety.

$$\mathrm{LCo} \underset{k_{-a}}{\overset{k_a}{\rightleftharpoons}} \mathrm{L} + \mathrm{Co} \tag{1}$$

$$\mathrm{L'} + \mathrm{Co} \xrightarrow{k_b} \mathrm{CoL'} \tag{2}$$

$$k_{(obsd)} = k_a \tag{3}$$

$$\mathrm{NH_2pyCo} \underset{k_r}{\overset{k_f}{\rightleftharpoons}} \mathrm{pyNH_2Co} \tag{4}$$

$$\mathrm{NH_2pyCo} \underset{k_{-1}}{\overset{k_1}{\rightleftharpoons}} \mathrm{NH_2py} + \mathrm{Co} \tag{5}$$

$$\mathrm{pyNH_2Co} \underset{k_{-1'}}{\overset{k_1'}{\rightleftharpoons}} \mathrm{NH_2py} + \mathrm{Co} \tag{6}$$

$$\mathrm{Co} + \mathrm{L'} \rightarrow \mathrm{CoL'} \tag{7}$$

$$k_{(obsd)} = \frac{k_1 + k_1'K}{1 + K},\ K = \frac{k_f}{k_r} \tag{8}$$

^{1}H NMR Line Shape Analysis. Dynamic ^{1}H NMR line shapes were simulated with the Nicolet program NMRXCH. Rate constants were determined by varying τ until the experimental and computer-simulated line shapes were visually identical. For further information see ref 9.

Analysis of Spin-Transfer NMR Data. Values for k_f were determined by analysis of the intensity vs. irradiation-time data collected for the oxime CH_3 signal of the endocyclic N-bound complex as the signal from the exocyclic N-bound complex was subjected to preacquisition radiofrequency saturation. Values for k_r were determined similarly by analysis of the oxime CH_3 ^{1}H NMR signal intensity vs. irradiation-time data obtained for the exocyclic N-bound complex. ^{1}H NMR signal intensity vs. time data were treated with the standard integrated expression for a first-order process by using linear least-squares analysis. The rate constants are defined in eq 4.

Preparations. All of the LCo(DH)$_2$R complexes were prepared from H$_2$OCo(DH)$_2$R by a published method.[16] The aquo complexes with R = CH_2CN and CH_2NO_2 were prepared from PhNH$_2$Co(DH)$_2$CH$_2$CN and (1,2-dimethylimidazole)Co(DH)$_2$CH$_2$NO$_2$, respectively, by treatment with strongly acidic ion exchange resin as described previously.[16]

(10) Rossi, M.; Glusker, J. P.; Randaccio, L.; Summers, M. F.; Toscano, P. J.; Marzilli, L. G. *J. Am. Chem. Soc.* **1985**, *107*, 1729.
(11) Bresciani-Pahor, N.; Forcolin, M.; Marzilli, L. G.; Randaccio, L.; Summers, M. F.; Toscano, P. J. *Coord. Chem. Rev.* **1985**, *63*, 1.
(12) Summers, M. F.; Toscano, P. J.; Bresciani-Pahor, N.; Nardin, G.; Randaccio, L.; Marzilli, L. G. *J. Am. Chem. Soc.* **1983**, *105*, 6259.
(13) Halpern, J., personal communication.
(14) Marzilli, L. G.; Summers, M. F.; Ramsden, J. H., Jr.; Bresciani-Pahor, N.; Randaccio, L. *J. Chem. Soc., Dalton Trans.* **1984**, 511.
(15) Martin, M. L.; Depluech, J.-J.; Martin, G. L. In *Practical NMR Spectroscopy*; Heyden: Lonon, 1980.
(16) Toscano, P. J.; Chiang, C. C.; Kistenmacher, T. J.; Marzilli, L. G. *Inorg. Chem.* **1981**, *20*, 1513.

Table I. Dissociation Rate Constants and Isomerization Equilibrium Constants for $2NH_2py\sim Co(DH)_2R$[a]

R	k_{obsd}, s^{-1}	% amino bound	K
CH_2NO_2	$3.8 \pm 0.1 \times 10^{-4}$	7	0.075
CH_2CF_3	$2.8 \pm 0.1 \times 10^{-2}$	10	0.111
CH_2Br	$1.5 \pm 0.1 \times 10^{-1}$ [b]	5	0.053
CH_3	3.5 ± 0.1 [b]	d	
$CH_2C(CH_3)(CO_2C_2H_5)_2$	$2.7 \pm 0.1 \times 10^{1}$	21	0.266
CH_2CH_3	$5.8 \pm 0.3 \times 10^{1}$ [b]	2	0.02
i-C_4H_9	$1.0 \pm 0.1 \times 10^{2}$ [b]	6	0.064
i-C_3H_7	c	17	0.205
CH_2OCH_3	c	2	0.02
neo-C_5H_{11}	c	18	0.219
adamantyl	c	46	0.855

[a] Rate and equilibrium data obtained in CH_2Cl_2 (25 °C) and CD_2Cl_2, respectively; see text for details. [b] From ref 12. [c] Too fast for stopped-flow measurements. [d] Not sufficiently soluble; see ref 12.

Table II. Dissociation Rate Constants ($R = CH_2CF_3$) and Isomerization Equilibrium Constants for $LCo(DH)_2R$[a] ($R = CH_2CF_3$ and i-C_3H_7)

	CH_2CF_3			i-C_3H_7	
L	10^2k_{obsd}, s^{-1}	% amino bound	K	% amino bound	K
$2NH_26CH_3py$	9.8 ± 0.3	100	$<10^2$		
$2NH_25CH_3py$	2.3 ± 0.1	28	0.389	54	1.174
$2NH_2py$	2.8 ± 0.1	10	0.111	17	0.205
$2NH_25NO_2py$		b	$\leq 10^{-2}$		
$2NH_24CH_3py$	1.3 ± 0.1	b	$\leq 10^{-2}$		
$2NH_23CH_3py$	3.1 ± 0.1	b	$\leq 10^{-2}$	b	$\leq 10^{-2}$

[a] See text for details. [b] None detected.

The compounds with $L = 2NH_26CH_3py$ and $2NH_26NH_2py$ were isolated as crystals from CH_2Cl_2/diethyl ether containing a 2:1 excess of L to Co. For elemental analyses (Atlantic Microlabs), see the supplementary material.

Crystal Data. The crystals of $py2NH_26NH_2Co(DH)_2CH_2CH_3 \cdot 2NH_26NH_2py$ were obtained as above. Cell parameters are as follows: space group = $P\bar{1}$, $a = 9.411$ (1) Å, $b = 10.276$ (1) Å, $c = 13.776$ (2) Å, $\alpha = 102.81$ (1)°, $\beta = 99.68$ (2)°, $\gamma = 81.85$ (1)°, $V = 1273.0$ Å^3, D(calcd) = 1.40 g cm^{-3}, D(measd) = 1.39, $Z = 2$ $C_{15}H_{26}CoN_7O_4 \cdot C_5H_7N_3$ units, mol wt = 536.6. The absorption coefficient μ is 7 cm^{-1} and the crystal dimensions are $0.03 \times 0.02 \times 0.02$ cm^3. Unit cell parameters were refined and intensity data collected on a CAD4 automated diffractometer with use of graphite-monochromated Mo Kα radiation, with standard procedures. A total of 6373 reflections up to $\theta = 28$ was collected; 3806 independent reflections having $I > 3\sigma(I)$ were corrected for Lorentz and polarization factors. Anomalous dispersion correction for non-hydrogen atoms was applied. No absorption correction was applied owing to the small size of the crystal used and the low value of the absorption coefficient.

Structure Determination and Refinement. The structure was solved by conventional Patterson and Fourier methods and refined by full-matrix anisotropic least-squares methods to the final R and R_w values of 0.043 and 0.054 respectively. The contribution of hydrogen atoms at the calculated positions, was held constant ($B = 5$ Å^2) and included in the final refinement. The final weighting scheme was $w = 1/(\sigma(F)^2 + (pF)^2 + q)$, where $p = 0.02$ and $q = 1$. Atomic scattering factors were those given in ref 17. All the calculations were done by using computer programs from the CAD4-SDP suite.

Results

Ligand Dissociation Rate Data. Results for the pseudo-first-order dissociation of L from $LCo(DH)_2R$ are given in Tables I and II. Values are the mean ± standard deviation for at least three data sets.

Equilibrium Data. Values of K (eq 4) are given in Tables I and II. For complexes with $R = CH_2CF_3$ and CH_2Br, values were obtained at 25 °C. For all other complexes, equilibrium concentrations were determined from the integrated ^{1}H NMR signals obtained at low temperature under slow-exchange conditions (for examples, see Figures 3 and 4 below). Equilibrium constants obtained in the absence of excess L were insensitive to temperature (−85 to +35 °C) within the limitations of the integration method.

Isomerization Rate Data. Rate data and activation parameters for isomerization (eq 4) are given in Table III. For $2NH_2py\sim Co(DH)_2CH_2CF_3$ ($\sim$ means ambidentate binding in solution), ^{1}H NMR line shape data were obtained from the oxime CH_3 signals of the isomers at temperatures from 27 to 40 °C. The rate constants at 25 °C were obtained by extrapolation of the ln k vs. $1/T$ data with use of linear least-squares analysis. Values of k at 25 °C for $2NH_2py\sim Co(DH)_2CH_2C(CH_3)(CO_2C_2H_5)_2$ were obtained similarly from −14 to 13 °C data. In all cases, chemical shifts in the exchange temperature region were obtained by extrapolation of the shift vs. T data obtained at stopped-exchange temperatures. For the data obtained in the presence of excess $2NH_2py$, equilibrium concentrations in the exchange temperature region were obtained by extrapolation of the ln K vs. $1/T$ data obtained at low temperatures.

Values of k in Table III which were obtained by using ^{1}H NMR spin transfer methods are the mean ± standard deviation for at least three sets of data.

Co–N Rotation Rate Data. Activation parameters and kinetic results for rotation of aminopyridines about the Co–N(endocyclic) bond for $LCo(DH)_2R$ complexes are given in Table IV. Examples of the dynamic ^{1}H NMR data obtained are given in Figures 1, 3, and 4 (below). For most complexes, values of T_2 (T_2 = transverse relaxation rate; see ref 9) were ~0.08 s. For complexes with $R = i$-C_3H_7 or C_2H_5, T_2 could not be determined directly due to high solution viscosity in the stopped-exchange temperature region (−90 °C, near the f.p. for CD_2Cl_2). Values of T_2 for these complexes were assumed to be 0.08 s.

The activation parameters and rate constants for rotation at −50 °C (Table IV) were determined by linear least-squares analysis of the ln k_{rot} vs. $1/T$ data.

Structural Results. The final positional parameters for $py2NH_26NH_2Co(DH)_2CH_2CH_3 \cdot 2NH_26NH_2py$ are given in Table V. Complete bond length and bond angles tables are given in the supplementary material. The atom numbering scheme is given in Figure 11 in the Discussion, where pertinent structural features will be described after consideration of the solution studies.

Discussion

Isomer Assignment. In our previous study of $2NH_2py$ and related cobaloximes, we were not able to obtain any evidence for exocyclic amino group bonding.[12] However, we obtained strong evidence for endocyclic N binding in sterically hindered 2R′NHpy compounds where R′ = CH_3, Bz. We will now review NMR results which establish the existence of ambidentate coordination by $2NH_2py$ and which permit the assignment of the bonding mode of the ligands.

Oxime O–H–O Signals. At high field (200 MHz) the O–H–O ^{1}H NMR signal is readily observed for alkyl cobaloximes.[11] These resonances occur with integration equivalent to 2 protons, are broad (~0.5 ppm full width at half height), and are very far downfield, ~17 to 18 ppm.

When a solution of $2CH_3NHpyCo(DH)_2CH_2CF_3$ is cooled, Figure 1, the O–H–O resonance first is narrowed ($T \sim 0$ °C), then broadened, and eventually resolved into two separate resonances of equal intensity. The X-ray structure of $2NH_2pyCo(DH)_2$-i-C_3H_7[12] reveals that one of the amino H atoms hydrogen bonds to an O atom of one of the O–H–O groups. Such H bonding would have the following effects: First, the rate of rotation about the Co–N bond would be decreased. Second, the O–H–O signals would become inequivalent if the rate of rotation and the chemical shift difference between the O–H–O signals were of appropriate magnitude. Third, one O in the O–H–O group involved in H bonding to the amino group would have weaker H-bonding interactions with the bridging H, and consequently the O–H–O signal would be displaced upfield (H bonding causes a downfield shift of H resonances. The observed changes in the NMR spectrum in the O–H–O region (Figure 1) are consistent with the processes just described.

(17) *International Tables of X-ray Crystallography*; Kynoch Press: Birmingham, 1974; Vol. IV.

Table III. Activation Parameters and Rate Data for Intramolecular Exchange between Exocyclic and Endocyclic Co–N Binding Modes in $LCO(DH)_2R$[a]

L	R	k_f, s^{-1}	k_r, s^{-1}	$E_a(k_f)$	ln $A(k_f)$
$2NH_2py$[b]	CH_2CF_3	$7.2 \pm 0.3 \times 10^{-1}$	4.4 ± 0.8		
$2NH_25CH_3py$[c]	CH_2CF_3	4.4×10^{-1}	1.13	29.96	49.76
$2NH_2py$	$CH_2C(CH_3)(CO_2C_2H_5)_2$	3.2×10^2	1.2×10^3	19.11	38.04
d	d	2.4×10^2	6.1×10^2	18.19	36.19

[a] CD_2Cl_2; values for *k* at 25 °C. [Cobaloxime] ~ 0.02 M. ^1H NMR line shape analyses performed unless otherwise noted. [b] Values determined by ^1H NMR saturation transfer. [c] Values for k_f and k_r determined by saturation transfer are 4.6×10^{-1} and 1.1 s^{-1}, respectively. [d] Data for $2NH_2pyCo(DH)_2CH_2C(CH_3)(CO_2C_2H_5)_2$ with 10-fold molar excess of $2NH_2py$.

Table IV. Activation Parameters and Rate Constants for Rotation of Aminopyridines about the Co–N Bond in $LCo(DH)_2R$[a]

	E_a, kcal mol^{-1}	ln *A*	k_{rot}(−50 °C), s^{-1}
	R = CH_2CF_3		
L			
$2NH_2py$	10.3	29.6	5.8×10^2
$2CH_3NHpy$	11.1	31.3	4.8×10^2
$2NH_25CH_3py$	13.4	36.4	4.7×10^2
$2NH_25NO_2py$	12.4	33.0	1.5×10^2
	L = $2NH_2py$		
R			
i-C_3H_7	9.2	30.3	1.4×10^4
CH_2CH_3[b]	9.5	30.3	7.0×10^3
neo-C_5H_{11}	10.2	30.8	2.4×10^3
CH_2Br	10.5	31.4	2.2×10^3
$CH_2C(CH_3)(CO_2C_2H_5)_2$	10.8	31.2	8.7×10^2
CH_2CN[c]	13.1	36.0	5.9×10^2
CH_2NO_2	9.5	27.4	3.9×10^2

[a] See text for details. A statistical treatment of the errors in rate and activation parameters for dynamic NMR data has been given; see: Binsch, G. In *Dynamic Nuclear Magnetic Resonance Spectroscopy*; Jackman, L. M., Cotton, F. A., Eds.; Academic Press: New York, 1975; p 45. From our previous studies, ref 12, the average deviation in *k* (Δk) is <20%. In this work, where the temperature range for line shape measurements (ΔT) is usually 50 deg for k_{rot}, the error associated with E_a is estimated as ≤13% (±1.3 kcal/mol). Note that errors in E_a and ln *A* tend to be mutually compensating. All solutions are ca. 0.02 M in cobaloxime. [b] The values for E_a, ln *A*, and k_{rot} (−50 deg) for L = $2CH_3NHpy$ at 9.8 kcal mol^{-1}, 31.6, and 8.3×10^3 s^{-1}, respectively. [c] Data obtained with a 10-fold molar excess of $2NH_2py$. The coalescence temperature in the presence and absence of excess $2NH_2py$ was the same.

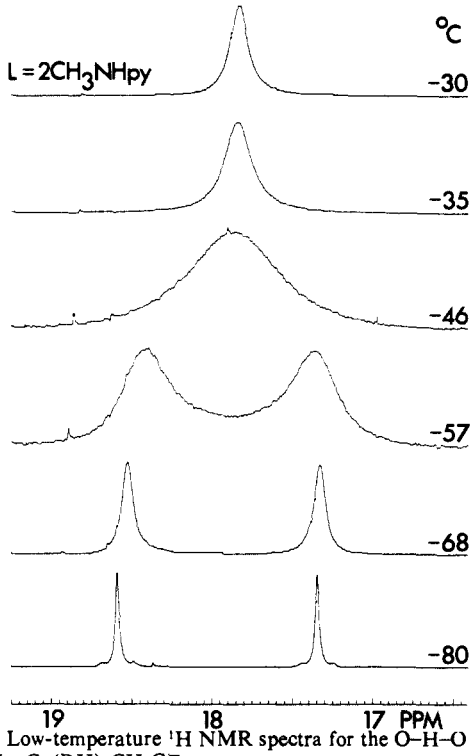

Figure 1. Low-temperature ^1H NMR spectra for the O–H–O signals of $2CH_3NHpyCo(DH)_2CH_2CF_3$.

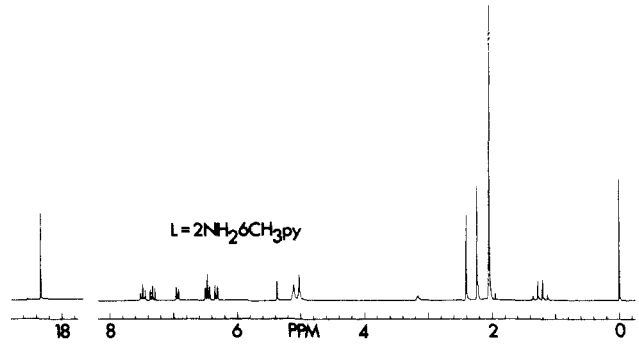

Figure 2. ^1H NMR spectrum of $py6CH_32NH_2Co(DH)_2CH_2CF_3$·$2NH_26CH_3py$ obtained at −90 °C.

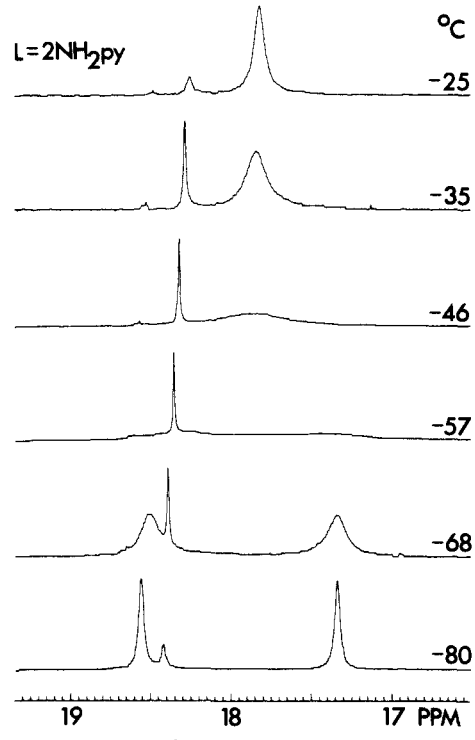

Figure 3. Low-temperature ^1H NMR spectra for the O–H–O signals of $2NH_2py{\sim}Co(DH)_2CH_2CF_3$.

A similar experiment with $py6CH_32NH_2Co(DH)_2CH_2CF_3$ (Figure 2) reveals no such broadening of the O–H–O signals on cooling. The chemical shift of this resonance is 18.62 ppm (*T* = −99 °C, Table V), consistent with the absence of amino group H bonding to the O–H–O groups. Steric arguments used previously[12] that $2NH_2$ 6-substituted py ligands are bound by the exocyclic amino group are supported by the X-ray structure and the more detailed steric considerations described below.

When $2NH_2py{\sim}Co(DH)_2CH_2CF_3$ is cooled (Figure 3), broadening of the O–H–O signal is observed as found for $2CH_3NHpyCo(DH)_2CH_2CF_3$ (Figure 1). However, part of the resonance remains as sharp as that observed for $py6CH_32NH_2Co(DH)_2CH_2CF_3$ (Figure 2). At −90 °C, the signals with chemical shifts of 17.33, 18.46, and 18.62 ppm are assigned to the O–H–O group of the endo isomer (endocyclic N

Table V. Atomic Positional Parameters of Non-Hydrogen Atoms with esd's in Parentheses for py2NH$_2$6NH$_2$Co(DH)$_2$CH$_2$CH$_3$·2NH$_2$6NH$_2$py

atom	x	y	z	atom	x	y	z
Co	0.20118 (5)	0.04389 (4)	0.30354 (3)	C7	0.3238 (4)	0.2778 (3)	0.3688 (3)
O1	−0.0545 (3)	0.1028 (3)	0.4018 (2)	C8	0.3437 (5)	0.4210 (4)	0.4153 (4)
O2	0.2914 (3)	−0.1993 (2)	0.1728 (2)	C9	0.3101 (4)	−0.0261 (4)	0.4247 (3)
O3	0.4596 (3)	−0.0243 (3)	0.2117 (2)	C10	0.3479 (9)	−0.1672 (6)	0.4202 (4)
O4	0.1136 (3)	0.2862 (2)	0.4348 (2)	C11	0.1439 (3)	0.1689 (3)	0.1167 (2)
N1	0.0262 (3)	0.0117 (3)	0.3386 (2)	C12	0.1743 (4)	0.2993 (3)	0.1314 (3)
N2	0.1884 (3)	−0.1318 (3)	0.2272 (2)	C13	0.2561 (5)	0.3281 (4)	0.0656 (3)
N3	0.3784 (3)	0.0720 (3)	0.2702 (2)	C14	0.3047 (4)	0.2292 (4)	−0.0088 (3)
N4	0.2145 (3)	0.2197 (3)	0.3791 (2)	C15	0.2663 (4)	0.1001 (4)	−0.0187 (3)
N5	0.0681 (3)	0.1277 (3)	0.1841 (2)	N8	0.1637 (3)	0.6121 (3)	0.7854 (2)
N6	0.1853 (3)	0.0698 (3)	0.0431 (2)	N9	0.0988 (4)	0.4969 (3)	0.6248 (3)
N7	0.3025 (4)	−0.0038 (4)	−0.0946 (3)	N10	0.2162 (4)	0.7317 (4)	0.9479 (2)
C1	−0.1595 (4)	−0.1413 (4)	0.3164 (3)	C16	0.1994 (4)	0.5133 (3)	0.7086 (3)
C2	−0.0220 (4)	−0.1020 (3)	0.2976 (3)	C17	0.3301 (4)	0.4294 (4)	0.7155 (3)
C3	0.0750 (4)	−0.1888 (3)	0.2309 (3)	C18	0.4218 (4)	0.4478 (4)	0.8051 (4)
C4	0.0497 (5)	−0.3278 (4)	0.1781 (4)	C19	0.3866 (4)	0.5462 (4)	0.8846 (3)
C5	0.5633 (4)	0.2266 (4)	0.2890 (3)	C20	0.2560 (4)	0.6261 (4)	0.8721 (3)
C6	0.4241 (4)	0.1882 (3)	0.3067 (3)				

Table VI. ^{1}H NMR δ Data for the O–H–O Signals of LCo(DH)$_2$R[a]

	endo		
	NH$_2$O–H–O[b]	O–H–O	exo O–H–O
	L = 2NH$_2$py		
R			
CH$_2$OCH$_3$	*b*	*b*	18.81
CH$_2$CH$_3$[c]	17.63	18.74	18.63
adamantyl	17.49	18.50	18.44
neo-C$_5$H$_{11}$	17.46	18.80	18.60
CH$_2$Br	17.42	18.61	18.48
i-C$_3$H$_7$	17.41	18.47	18.57
CH$_2$CF$_3$	17.33	18.62	18.46
CH$_2$C(CH$_3$)(CO$_2$C$_2$H$_5$)	17.27	18.67	18.53
CH$_2$NO$_2$	17.18	18.48	18.31
	R = CH$_2$CF$_3$		
L			
2NH$_2$6CH$_3$py	*d*	*d*	18.62
2CH$_3$NHpy	17.35	18.65	*d*
2NH$_2$5CH$_3$py	17.34	18.65	18.41
2NH$_2$py	17.33	18.62	18.46
2NH$_2$5NO$_2$py	17.07	18.66	*d*

[a] −95 to −70 °C. [b] Stopped-exchange (Co–N rotation) spectra unobtainable in CD$_2$Cl$_2$. [c] A single, sharp resonance at 18.34 ppm was observed for py2NH$_2$6NH$_2$Co(DH)$_2$CH$_2$CH$_3$·2NH$_2$6NH$_2$py. [d] None detected.

binding) H bonded to the NH$_2$ group, the two equivalent O–H–O groups of the exo isomer (exocyclic N binding), and the O–H–O group of the endo isomer not H bonded to the amino group.

In Table VI. we summarize the O–H–O signals for several compounds. As the nature of the substituents on py changes or as the R group changes, the intensities of signals assignable to endo and exo isomers usually change in a readily understood manner (Figure 4).

These O–H–O signals are an important method for detecting small amounts of exo isomer since the endo isomer signals are very broad near coalescence. The observation of small amounts of endo isomer is difficult in situations where the exo isomer predominates. Therefore, we place less confidence on the absence of the endo isomer in the py6CH$_3$2NH$_2$ compound (Table II) than on the absence of the exo isomer for the bottom three entries in Table II.

Oxime CH$_3$ Signals. The ^{1}H NMR signals for the oxime CH$_3$ groups undergo changes similar to those described above for the O–H–O signals. However, unlike the situation for the broad O–H–O signals, separate signals are observed for the exo and endo isomers at room temperature for complexes with R = CH$_2$CF$_3$, CH$_2$X (X = Cl, Br, I), and CH$_2$NO$_2$. Complexes with other alkyl groups give only one signal at room temperature due to ligand isomerization which is fast on the NMR time scale (Figure 5).

Chemical shifts for the exo and endo isomers of the slow-exchange compounds are ~2.05 and ~2.25 ppm, respectively. The upfield shifts for the exo isomers may be due to the anisotropic effect of the aromatic pyridine ring which is oriented above the

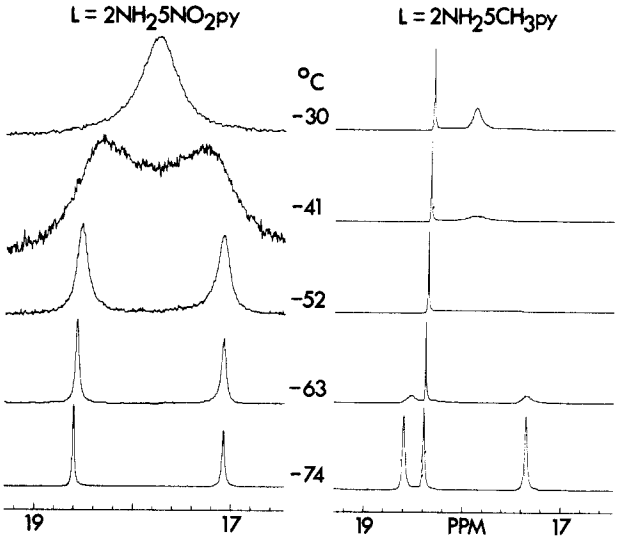

Figure 4. Low-temperature ^{1}H NMR spectra for the O–H–O signals of LCo(DH)$_2$CH$_2$CF$_3$ (L = 2NH$_2$5NO$_2$py and 2NH$_2$5CH$_3$py).

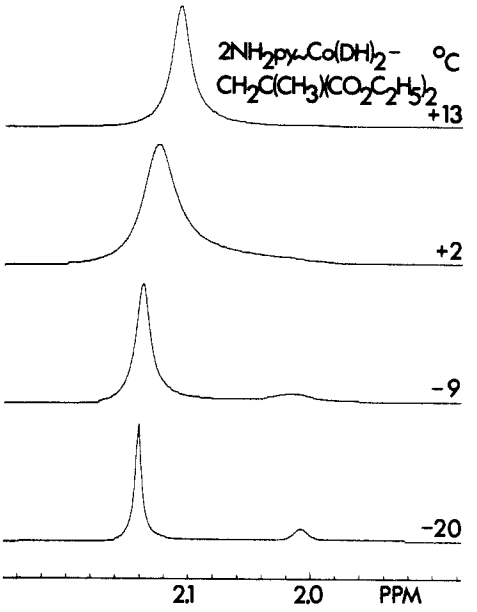

Figure 5. ^{1}H NMR spectra for the oxime CH$_3$ signals of 2NH$_2$py~Co(DH)$_2$CH$_2$C(CH$_3$)(CO$_2$C$_2$H$_5$)$_2$. The upfield signal is from the exo isomer.

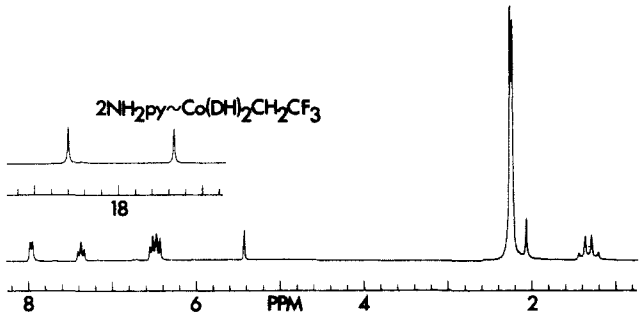

Figure 6. ^{1}H NMR spectrum for 2NHpy~Co(DH)$_2$CH$_2$CF$_3$ obtained at −90 °C. The two larger downfield peaks at 2.23 and 2.25 ppm and the small peak at 2.05 ppm are due to the oxime CH_3 of the endo and exo isomers, respectively. The O–H–O signal for the latter has become very broad at this temperature.

oxime CH_3 groups in the exo isomer. In general, chemical shifts for complexes with L = aliphatic N donors are downfield from complexes with L = aromatic N donors. However, for L = aniline derivatives, upfield shifts are obtained. For example, for 29 cobaloximes surveyed with R = i-C_3H_7, mean values of chemical shifts (± standard deviation) for the oxime CH_3 are 2.11 ± 0.03 ppm for 10 complexes with aromatic N donors, 2.26 ± 0.03 ppm for 13 complexes with aliphatic N donors, and 2.06 ± 0.04 ppm for 6 complexes containing substituted anilines.[11]

Upon cooling, in all cases where an exo–endo equilibrium was observed from the O–H–O signals, two signals of appropriate intensity and chemical shift were also obtained for the oxime CH_3 groups (Figure 5). At very low temperatures (−75 to −90 °C) it was also possible to observe splitting of the endo signal due to slow rotation about the Co–N bond (Figure 6).

Exo–Endo Equilibrium. Numerous factors influence the position of the exo–endo equilibrium. The data in Tables I and II illustrate some trends.

Effect of L. Variation of the substituents on L leads to changes in K which are readily understood on the basis of either steric effects or electronic effects. For example, substitutions which increase electron donation by the endocyclic N will favor the endo isomer whereas a substituent at the 6 position will sterically block formation of this isomer. Likewise, a substituent on the amine group will sterically interfere with formation of an exo isomer.[12] Substitution of one amino hydrogen as mentioned above or placing a CH_3 group at the 3-position greatly, if not completely, favors the endo isomer. Substitution at the 6 position greatly favors the exo isomer (Figure 2). Electron donating groups at the 4 position or electron withdrawing groups at the 5 position favor the endo isomer. Electron donating groups at the 5 position somewhat favor the exo isomer. The spectra in Figure 4 clearly illustrate these effects (K values for R = CH_2CF_3 and L = 2NH$_2$5NO$_2$py and 2NH$_2$5CH$_3$py are $\leq 10^{-2}$ and 0.389, respectively, Table II).

Effect of R. Variation in the R group could, in theory, influence the equilibrium in many, sometimes conflicting, ways. Increased electron donation to the Co(DH)$_2$ system by good electron donating R groups (a) increases the H-bonding ability of the oxime O atoms and (b) leads to lengthening of the trans Co–N bond.[11] In theory, both of these electronic effects could lead to increased endo binding.[12]

^{13}C NMR chemical shifts for the γ(py) carbon of pyCo(DH)$_2$R complexes are particularly sensitive to changes in the electron donating ability of R.[11,18] In Figure 7 the equilibrium constant K (eq 8) for 2NH$_2$py~Co(DH)$_2$R is plotted against the γ(py) ^{13}C NMR chemical shift for pyCo(DH)$_2$R. It is clear from these data that there is no straightforward relationship between K and ^{13}C shifts; thus it appears that K is relatively insensitive to the inductive nature of R. This lack of dependence on R is somewhat surprising since the equilibrium constant (K_a) for proton dissociation from O–H–O increases by 3 orders of magnitude in going from R = i-C_3H_7 to CH_2CN,[19] and Co–N(py) bond lengths[20,21] increase from 2.028 to 2.099 Å for R = CH_2NO_2 and i-C_3H_7, respectively.

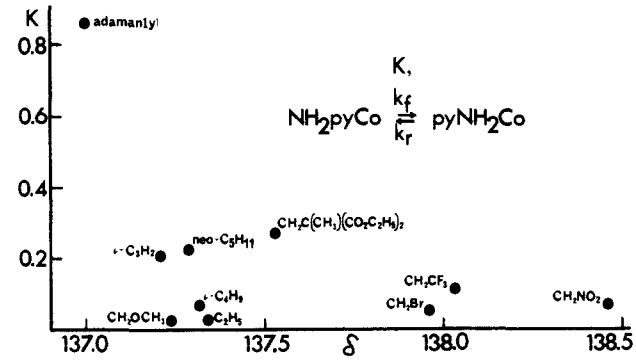

Figure 7. Plot of K for 2NH$_2$py~Co(DH)$_2$R vs. ^{13}C NMR δ for the γ(py) carbon of pyCo(DH)$_2$R (R = (left to right) adamantyl, i-C_3H_7, CH_2OCH_3, neo-C_5H_{11}, i-C_4H_9, CH_2CH_3, $CH_2C(CH_3)(CO_2C_2H_5)_2$, CH_2Br, CH_2CF_3, and CH_2NO_2).

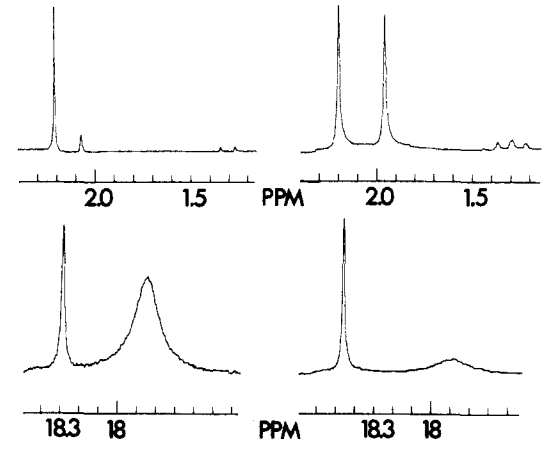

Figure 8. Upfield (top) and downfield regions of the ^{1}H NMR spectrum for 2NH$_2$py~Co(DH)$_2$CH$_2$CF$_3$ (~0.02 M) (T = −33 °C). The singlets at 2.21 and 2.07 ppm are due to the oxime CH_3 of the endo and exo isomer, respectively, and the quartet at ~1.3 ppm is due to the CH_2CF_3 group. The sharp signal at 18.30 ppm and the broad signal at 17.85 ppm are due to the O–H–O groups of the exo and endo isomer, respectively. The spectral regions on the right are for a solution with a 20-fold excess of 2NH$_2$py.

It appears that K is influenced less by inductive effects than by the steric trans influence of bulky R groups (e.g., R distorts the Co(DH)$_2$ moiety and increases steric interactions between L and Co(DH)$_2$).[22] Values of K for R = adamantyl, i-C_3H_7, neo-C_5H_{11}, and $CH_2C(CH_3)(CO_2C_2H_5)_2$ are 0.855, 0.205, 0.219, and 0.266, respectively, compared to values of K for the less bulky alkyls of 0.020 to 0.111 (Table I). This is not altogether surprising, considering the following argument. Bulky R groups should have a greater influence on k_f relative to k_r, since endocyclic N-bound 2NH$_2$py probably experiences greater contact with the (DH)$_2$ unit than does exocyclic N-bound 2NH$_2$py. Greater-than-expected dissociation rates for compounds with bulky R groups including R = i-C_3H_7 can be attributed to a steric effect.[23,24] The relative

(18) Stewart, R. C.; Marzilli, L. G. *Inorg. Chem.* **1977**, *16*, 424. See Zangrando et al. (Zangrando, E.; Bresciani-Pahor, N.; Randaccio, L.; Charland, J. P.; Marzilli, L. G. *Organometallics*, submitted) for the most recent correlation.

(19) Brown, K. L.; Lyles, D.; Pencovici, M.; Kallen, R. G. *J. Am. Chem. Soc.* **1975**, *97*, 7338.

(20) Randaccio, L.; Bresciani-Pahor, N.; Toscano, P. J.; Marzilli, L. G. *Inorg. Chem.* **1981**, *20*, 2722.

(21) Marzilli, L. G.; Toscano, P. J.; Randaccio, L.; Bresciani-Pahor, N.; Calligaris, M. *J. Am. Chem. Soc.* **1979**, *101*, 6754.

(22) One measure of such distortion is the "butterfly" bending between the (DH)$_2$ planes as defined by the detached angle α. For a discussion of α see ref 11; see also: Bresciani-Pahor, N.; Randaccio, L.; Toscano, P. J.; Sandercock, A. C.; Marzilli, L. G. *J. Chem. Soc., Dalton Trans.* **1982**, 129.

(23) Unpublished results from these laboratories.

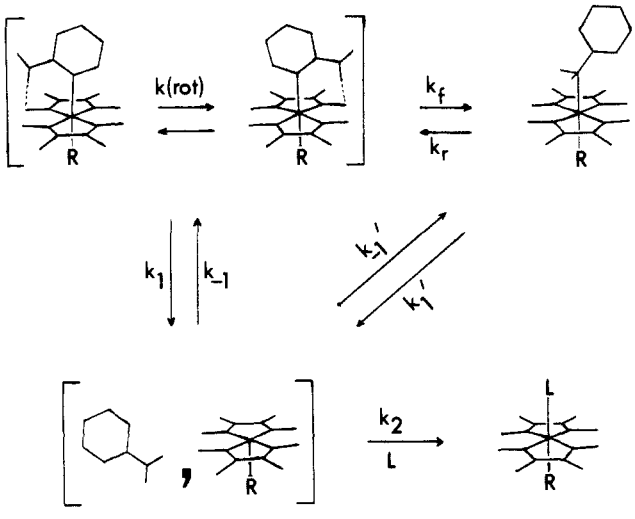

Figure 9. Scheme depicting the solution behavior of $2NH_2py$-containing cobaloximes.

kinetic steric effect on endo and exo N-bound $2NH_2py$ may be the most important factor governing the position of equilibrium for complexes with different R groups.

If shorter Co–N bonds produced greater steric interactions, values of K would be expected to increase. However, values of K and Co–N(py) bond lengths for R = CH_2NO_2 and C_2H_5 are 0.075, 2.028 (3) Å and 0.020, 2.084 (7) Å, respectively.[20,25] This finding suggests a greater preference of $Co(DH)_2R$ for the more basic donor (endocyclic N) as the electron donating ability of R decreases. Such a preference would counteract the steric effect of shorter Co–N bonds and explain the lack of dependence of K on R electron donor properties. No detailed information concerning such preference has been reported.

Effect of Excess L. One of the most unusual observations we have made concerning the exo–endo equilibrium involves the effect of added $2NH_2py$. In Figure 8, we show the oxime O–H–O and CH_3 region of $2NH_2py{\sim}Co(DH)_2CH_2CF_3$ nT = −33 °C). With addition of a 20-fold excess of $2NH_2py$ (Figure 8), the percentage of exo isomer increases to ~50%. An increase was also observed for complexes with other R groups. An explanation for this unusual and unique observation is that the added $2NH_2py$ H bonds to the O–H–O groups or the coordinated NH_2 group. Interestingly, as $2NH_2py$ is added, chemical shifts for the O–H–O and CH_3 groups of the exo isomer move to lower and higher fields, respectively, while shifts for the endo isomer are less affected. Also, the value for k_r is much smaller with addition of $2NH_2py$ (Table III). The value of k_f is also slightly reduced. These data and the fact that added $2NH_2py$ does not affect k_{rot} indicate that the added $2NH_2py$ probably interacts with the exo isomer.

Dynamic Properties. Three different rate processes (ligand exchange, isomerization, and ligand rotation) were evaluated (Figure 9). We will consider the relationship between exchange and isomerization rates together.

Ligand Exchange and Isomerization Rates. Ligand exchange reactions have been studied for a large variety of cobaloxime derivatives and, in noncoordinating solvents, ligand substitution proceeds via an S_N1 LIM mechanism (eq 1–3).[11,12,24,26] For such a process, the rate-limiting step is L dissociation and the resulting 5-coordinate intermediate is highly reactive.[26] Dissociation rates ($k_{obsd} = k_a$) and competition ratios (k_{-a}/k_b) which reflect the relative reactivity of incoming ligands toward the 5-coordinate intermediate, have been previously determined for some aminopyridine-containing cobaloximes.[12] In earlier studies we have shown that $2NH_2py$ is more labile than 4CNpy by a factor of ~75 ± 15 and that $2NH_2py$ is a better competitor than 4CNpy.

For all ligand substitution data obtained here, plots of ln ($A - A_\infty$) vs. t were linear, and in no cases was curvature, which might indicate parallel reactions, obtained. To test for rapid L isomerization prior to dissociation, the displacement of $2NH_25CH_3py$ from $2NH_25CH_3py{\sim}Co(DH)_2CH_2CF_3$ (~0.02 M) by $P(OCH_3)_3$ (10-fold molar excess) was monitored by ^1H NMR spectroscopy at 13 °C. The oxime CH_3 signals of the exo and endo isomers of the $2NH_25CH_3py$ complex were monitored for a period of ~3 min; subsequently, only the $P(OMe)_3$ derivative could be observed. The ratio of the two isomers was constant throughout the reaction.

Isomerization rate constants were determined for some of the cobaloximes via dynamic and saturation-transfer ^1H NMR spectroscopy. The compounds chosen for study were those which (1) had values of $K > 0.1$, (2) gave clearly resolved signals for the endo and exo species, and (3) had measurable dissociation rates. In all cases isomerization rates exceeded dissociation rates by at least an order of magnitude (Table I–III). Thus, ambidentate isomerization is mainly an intramolecular process with only a small contribution from ligand exchange processes as given by eq 4–8 and depicted in Figure 9 (with L = L′).

For all compounds studied, changes in k_{obsd} as R is varied follow the usual reactivity patterns already observed[11,24,26,27] for a variety of other L; e.g., k_{obsd} increases by a factor of ~2 × 10^3 when CH_2CF_3 is replaced by CH_2CH_3 (Table I).

Values of k_{obsd} for $LCo(DH)_2CH_2CF_3$, where L = substituted aminopyridines including $2NH_2nCH_3py$ (n = 3, 4, 5, 6), are given in Table II. One striking feature which emerges from these data is that values of k_{obsd} for all the complexes differ by less than an order of magnitude. This is especially intriguing since k_{obsd} for $2CH_3pyCo(DH)_2CH_3$ is greater than k_{obsd} for $pyCo(DH)_2CH_3$ by a factor of ~10^4![12] Although changes in k_{obsd} are relatively small, changes in K are large; measured values of K for L = $2NH_23CH_3py$ and $2NH_26CH_3py$ are $\leq 10^{-2}$ and $\geq 10^2$, respectively. Thus the dissociation rate constants (k_1 and k_1') are probably similar for the endocyclic and exocyclic N-bound $2NH_2py$ derivatives; and, whereas placing a CH_3 group on the α-carbon of py greatly accelerates the leaving rate of this ligand, placing a CH_3 group on C-6 of $2NH_2py$ shifts the equilibrium to amino group binding, with only a minor increase in k_{obsd}.

Although it was not possible to determine k_1 and k_1' directly, approximate values may be estimated from the data in Table II as follows. Values of k_{obsd} and K for $2NH_26CH_3py$ and $2NH_23CH_3py$ (R = CH_2CF_3) are 9.8 × 10^{-2} s^{-1} and $\geq 10^2$, and 3.1 × 10^{-2} s^{-1} and $\leq 10^{-2}$, respectively. For $2NH_26CH_3py$, the m-CH_3 substituent should have only minor electronic and steric effects on the strength of exocyclic N binding; likewise, for $2NH_23CH_3py$ the m-CH_3 group should not have much effect on the nature of the Co-to-endocyclic N bond. For both ligands, however, the CH_3 group acts as a steric block for one of the potential binding atoms. Thus values of k_1 and k_1' for L = $2NH_2py$ and R = CH_2CF_3 may be crudely estimated as ~3 × 10^{-2} and ~1 × 10^{-1} s^{-1}, respectively. Note, however, that these approximations do not take into account the effect of the CH_3 group on the H-bonding ability of the NH_2 group which may also affect k_{obsd}.

Co–N(endo) Rotation Rates. In Figure 10, values of log k_{rot} for $2NH_2pyCo(DH)_2R$ complexes are plotted against ^{13}C NMR shifts for the γ(py) carbon of $pyCo(DH)_2R$ complexes. In general, as rotation rates increase, the ^{13}C NMR resonances shift to higher field. This plot (Figure 10) contains a great deal of scatter which may be due to a number of possibly counteracting factors. Thus, good electron-donating R groups would be expected to increase k_{rot} by lengthening and labilizing the Co–N bond and to decrease k_{rot} by making the oxime O atoms better H bond acceptors.

For R = CH_2CF_3 and L = $2NH_25CH_3py$ or $2CH_3NHpy$, there is little difference in k_{rot} compared to $2NH_2py$. However, when L = $2NH_25NO_2py$, where the Co–N bond should be weaker and intramolecular H bonding should be stronger than in the $2NH_2py$ compound, k_{rot} is somewhat smaller, possibly demonstrating the effect of H bonding.

(24) Ramsden, J. H., Jr., Ph.D. Thesis, the Johns Hopkins University, 1980.
(25) Simonov, Yu. A.; Skurpelo, A. J.; Camus, N. M.; Belokoneva, E. L.; Camus, J. D. *Koord. Chim.* (*Russian*) **1980**, 6, 1107.
(26) Stewart, R. C.; Marzilli, L. G. *J. Am. Chem. Soc.* **1978**, *100*, 817.
(27) Brown, K. L.; Awtrey, A. W. *Inorg. Chem.* **1978**, *17*, 111.

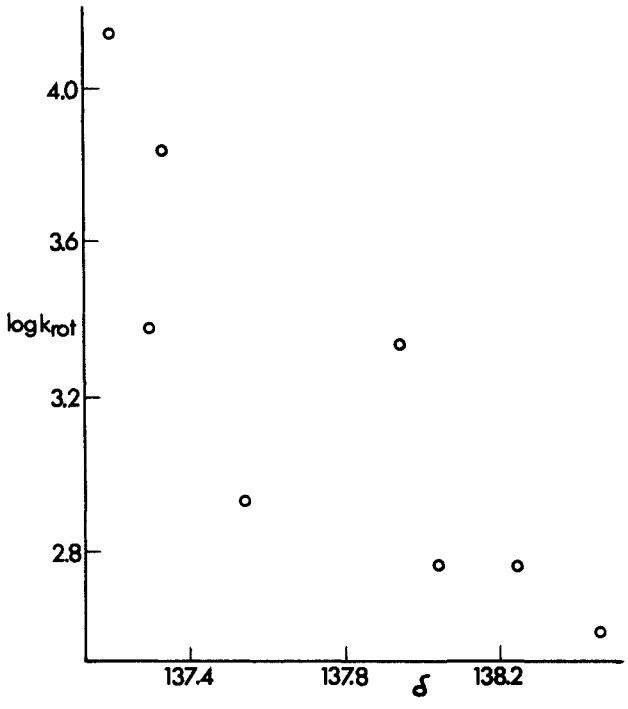

Figure 10. Plot of log k_{rot} for $2NH_2pyCo(DH)_2R$ vs. ^{13}C NMR δ for the γ(py) carbon of $pyCo(DH)_2R$ (R = (left to right) *i*-C_3H_7, *neo*-C_5H_{11}, CH_2CH_3, $CH_2C(CH_3)(CO_2C_2H_5)_2$, CH_2Br, CH_2CF_3, CH_2CN, and CH_2NO_2).

Comparison of Structural and Solution Results. In a previous study,[12] we assumed that a 2-amino 6-substituted pyridine could bind only via the exocyclic amino group. The ^1H NMR data described above provide extremely strong evidence for this conclusion. Attempts at obtaining suitable crystalline complexes with ligands such as $2NH_26CH_3py$ have failed. In general, when 2-aminopyridine contains 6-substituents which force exocyclic amino group coordination, solids are obtained with excess ligand present. One example of the latter was crystallized, namely $py2NH_26NH_2Co(DH)_2CH_2CH_3{\cdot}py2NH_26NH_2$. The ORTEP drawing and atom numbering scheme for the crystallographically independent adduct, $py2NH_26NH_2Co(DH)_2CH_2CH_3{\cdot}py2NH_26NH_2$, is given in Figure 11.

The $Co(DH)_2$ moiety is nearly planar with an angle of 4° between the planes passing through the atoms of each DH unit. The four N equatorial atoms are coplanar within ±0.01°. The cobalt atom is displaced out of this mean plane by 0.01 Å toward the neutral ligand. The axial N–Co–C fragment is characterized by Co–C and Co–N distances of 2.025 (3) and 2.156 (3) Å, respectively, and by a N–Co–C angle of 174.1 (1)°. The Co–CH_2–CH_3 angle is 121.0 (3)° and the CH_2–CH_3 bond length is 1.434 (6) Å. The shortening of the latter bond as well as the widening of the Co–C–C angle is typical of Co–CH_2R moieties in cobaloximes.[28]

These values adhere to a trend in which the CH_2–CH_3 bond length decreases and the Co–C–C bond angle increases as L bulk increases (e.g., 1.519 (8) Å and 117.8 (4)° for L = 4(MeO)C(NH)py;[14] 1.479 (6) Å and 117.8 (3)° for L = $PhNH_2$;[23] 1.317 (9) Å and 126.2 (5)° for L = Ph_3P[28]). No significant trend is observed for Co–C bond lengths, however.

The C(9)–C(10) bond is nearly above the Co–N(2) equatorial bond while the N(5)–C(11) bond is nearly above the Co–N(3) bond. The Co–N(5)–C(11) angle of 115.9 (2)° is close to that of 118.1 (2)° found in the $PhNH_2$ analogue and suggests that no dramatic steric interactions between these axial ligands and the equatorial moiety occur. The Co–N(5) bond of 2.156 (3) Å is very close to that of 2.147 (2) Å found in the latter analogue. A comparison between other pyridine[11] and aniline alkyl cobaloximes[23] indicates that the Co–py bond length is about 0.07 Å shorther than the Co–aniline distance. Such a difference can be attributed mainly to the larger radius of a sp^3-hybridized N over an sp^2-hybridized N. This expected shorter Co–N distance for endo coordination contrasts with an estimated value of ca. 2.7 Å for an endo-coordinated $2NH_26NH_2py$ (A below). This hypothetical structure is compared with that of $2NH_2pyCo(DH)_2iC_3H_7$ (B). A bond distance of 2.7 Å virtually excludes any endo coordination by $2NH_26NH_2py$. Indeed, the ^1H NMR data for $py2NH_26NH_2Co(DH)_2CH_2CH_3{\cdot}py2NH_26NH_2$ are in excellent agreement with values expected for exo coordination. For example, exo-coordinated 2-aminopyridine. Additionally, the O–H–O signal at 18.34 ppm is slightly upfield to that expected for exo coordination, but a small upfield shift is expected from the interaction with the free $2NH_26NH_2py$. The signal remains sharp, even at very low *T* (Table VI). This result is also consistent with exclusive exo binding. Finally, the solid-state structure reveals H-bonding interactions between the uncoordinated $2NH_26NH_2py$ and the complex. The uncoordinated $2NH_26NH_2py$ makes short contacts, consistent with hydrogen bonding as follows: N(9)···O(4) of 3.01 Å; N(9)···O(4)′ of 2.94 Å, where O(4)′ is related to O(4) by the center of symmetry at $0,0,{}^1/_2$; and N(10)···O(2)′ of 3.04 Å, where O(2)′ is translated by $z = 1$ and $y = 1$.[29] This result is in agreement with our observation of the unusual dependence of ambidentate ligand coordination mode on the presence of excess ligand. Presumably, the propensity for H-bonding interaction in

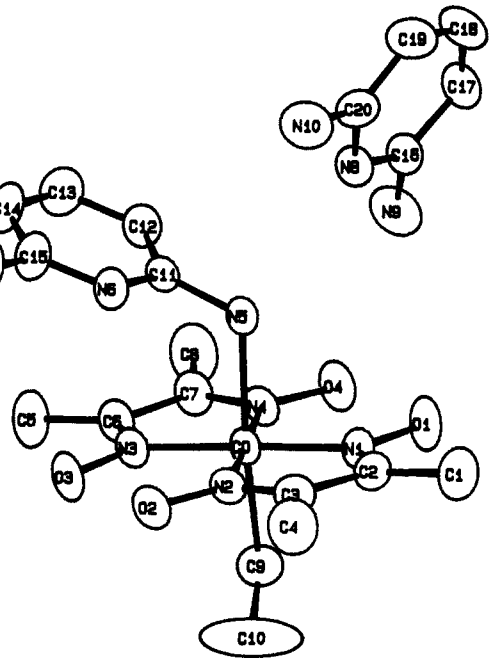

Figure 11. Structure and atom labeling scheme for non-hydrogen atoms (thermal ellipsoids, 50% probability) for $py2NH_26NH_2Co(DH)_2CH_2CH_3{\cdot}py2NH_26NH_2$.

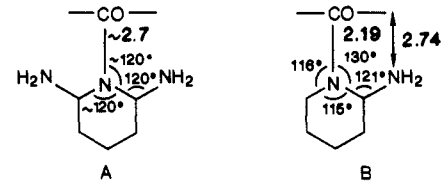

(28) Randaccio, L.; Bresciani-Pahor, N.; Orbell, J. D.; Calligaris, M.; Summers, M. F.; Snyder, B.; Toscano, P. J.; Marzilli, L. G. *Organometallics* **1985**, *3*, 469. Bresciani-Pahor, N.; Randaccio, L.; Summers, M.; Toscano, P. J. *Inorg. Chim. Acta* **1983**, *68*, 69.

(29) Intermolecular distances do not suggest any involvement of the coordinated NH_2 group in H-bonding. Shortest N–N distances are 3.20 and 3.31 Å to N(8) and N(10), respectively. However, the other NH_2 of the ligand probably interacts with the $Co(DH)_2$ units of a molecule related by the symmetry center at ${}^1/_2,0,0$. The N(7)···O(3)′ distance is 3.00 Å.

the amino-bound form hinders isolation of crystalline product in the absence of excess ligand.

Relevance to B_{12} Chemistry and Biochemistry. Model studies reveal that steric interactions between bulky R groups and equatorial ligands weaken Co–C bonds as evidenced by longer[11] and weaker Co–C bonds.[3-6] Similarly, cobalamins with bulky R groups have less stable Co–C bonds.[2,30-32]

Comparisons of the structures of coenzyme B_{12} (5'-deoxyadenosylcobalamin) and MeB_{12} (methylcobalamin with each other and with models reveal no unusual structural features.[7,9,10] Indeed, Co–C bond cleavage in coenzyme B_{12} requires a conformational change induced by the enzyme.[1] A feasible change is a protein-induced distortion which increases steric repulsion between the corrin and the deoxyadenosyl and/or Co–C–C or N–Co–C bond angle deformations.[1,2,10,30-34]

The importance of such steric interactions has been clearly demonstrated for cobaloximes with trans P-donor ligands where the equatorial $Co(DH)_2$ system is distorted toward R.[11] However, from trans N-donor ligands, large distortions are not found with any regularity except for very bulky R where the distortion is toward the N donor.[11]

In cobalamins with bulky R, the "base off" forms (pendant 5,6-dimethylbenzimidazole, 5,6DMBz) are relatively stable but the "base on" forms are very unstable to Co–C bond cleavage.[31,32] Similarly, bulky R groups promote dissociation of 5,6DMBz and thus stabilize the "base off" form, which is believed to be five coordinate.[31,32] This information together could be taken to suggest that the 5,6DMBz distorts the corrin and thereby weakens the Co–C bond.[31]

However, there are some problems with such an interpretation. First, the bulky R groups studied are also good trans labilizers.[32] The "base off" form is favored by good trans labilizer ligands regardless of bulk.[32] Thus, the electronic and steric effects are not easily separated. Second, Co–C bond homolysis of such "base off" cobalamins would form an unstable four-coordinate cobalt(II) species (presumably through an incipient four-coordinate cobalt(II) activated complex).[33] Thus, the steric effect of the 5,6DMBz may be limited to maintaining the Co in the equatorial corrin N_4 plane.[32,33,35] Our observation, that the value of K (eq 4 and 8) is not dependent on the electronic properties of R (as judged by Co–N bond distances, ^{13}C shifts, etc.) but on the bulk of R, is the first clear evidence for a steric effect of R on N-donor binding in solution.

A picture which is emerging from the ongoing studies in several laboratories is that the 5,6DMBz's major role is to maintain Co in the corrin N_4 plane and to stabilize the cobalt(II) intermediate.[33] Additional distortions caused by the enzyme could include (a) Co–C–C and/or N–Co–C bond distortion, (b) corrin ring deformation, (c) Co–N (5,6DMBz) bond lengthening, or (d) a combination of (a) → (c). Although the most obvious corrin ring distortion would involve enhanced interaction with the 5'-deoxyadenosyl, it is conceivable that the Co–N(5,6DMBz) bond could also be lengthened.[9,12] Additional experimental and theoretical studies on models, cobalamins, and enzymic systems are clearly needed to help resolve these issues.

Acknowledgment. This work was supported by NIH Grant GM 29225 to L.G.M. and a grant from MPI (Rome) to L.R. L.G.M. thanks the Alexander von Humboldt Foundation for a Senior U.S. Scientist Award. The NSF aided in the purchase of the 360-MHz NMR instrument.

Supplementary Material Available: Tables of elemental analyses, bond lengths, and bond angles, hydrogen atom coordinates, anisotropic thermal parameters, and calculated and observed structure factors (21 pages). Ordering information is given on any current masthead page.

(30) Christianson, D. W.; Lipscomb, W. N. *J. Am. Chem. Soc.* **1985**, *107*, 2682.
(31) Schrauzer, G. N.; Grate, J. H. *J. Am. Chem. Soc.* **1981**, *103*, 541. Grate, J. H.; Grate, J. W.; Schrauzer, G. N. *J. Am. Chem. Soc.* **1982**, *104*, 1588. Grate, J. H.; Schrauzer, G. N. *J. Am. Chem. Soc.* **1979**, *101*, 4601.
(32) Chemaly, S. M.; Pratt, J. M. *J. Chem. Soc., Dalton Trans.* **1980**, 2259.
(33) Marzilli, L. G.; Summers, M. F.; Bresciani-Pahor, N.; Zangrando, E.; Charland, J.-P.; Randaccio, L. *J. Am. Chem. Soc.* **1985**, *107*, 6880.
(34) Halpern, J. *Ann. N.Y. Acad. Sci. (U.S.A)* **1974**, *239*, 2.
(35) A reviewer has pointed out that the 5,6-DMBz coordination causes folding of the corrin. A second reviewer questions the view that the "base off" species is five coordinate and suggests a six-coordinate aquo species as a more likely alternative. We agree that the nature of the "base off" cobalamin is presently not understood and that the spectral evidence for a five-coordinate species has alternative explanations. However, we also feel that there are good reasons, independent of the spectral evidence, for suggesting the existence of five-coordinate organo cobalamins. This issue clearly needs resolution.

A Flash Photolysis Investigation of Dihydrogen Elimination from Phosphine Complexes of Iridium(III) and Rhodium(III): $H_2IrCl(CO)(PPh_3)_2$, $H_2IrCl(PPh_3)_3$, and $H_2RhCl(PPh_3)_3$

David A. Wink and Peter C. Ford*

Contribution from the University of California, Santa Barbara, Santa Barbara, California 93106. *Received December 18, 1985*

Abstract: Flash photolysis studies of the two iridium(III) dihydride complexes $H_2IrCl(L')(PPh_3)_2$ (L' = CO or PPh_3) in deaerated benzene solution demonstrate the formation of a common intermediate $IrCl(PPh_3)_2$ for each case. This species reacts with CO and PPh_3 to form $IrCl(CO)(PPh_3)_2$ and $IrCl(PPh_3)_3$ with the respective rate constants 2.5×10^8 and 1.3×10^7 M^{-1} s^{-1}. A model is proposed by which the primary photoreaction in these cases is ligand dissociation to give the common five-coordinate intermediate $H_2IrCl(PPh_3)_2$ which undergoes rapid dihydrogen elimination to give $IrCl(PPh_3)_2$ in competition with back reaction with L'. Continuous photolysis in the presence of added L' reduced quantum yields for dihydrogen loss in a manner consistent with this model. The dramatically enhanced rate of H_2 elimination from the pentacoordinate intermediate (relative to the hexacoordinate analogues) would be consistent with theoretical treatments of this process based on orbital topology changes. The rhodium(III) dihydride $H_2RhCl(PPh_3)_3$ undergoes a different photoreaction pathway, concerted dihydrogen elimination, to give the tetracoordinate species $RhCl(PPh_3)_3$ as the primary photoproduct. These results indicate the multiplicity of reaction channels available to the electronic excited states of such complexes.

The photochemical excitation of transition metal di- and polyhydrides generally is accompanied by the reductive elimination of dihydrogen to give a coordinatively unsaturated metal-containing product, e.g.,

0002-7863/86/1508-4838$01.50/0